NMR Investigation of β-Substituted High-Spin and Low-Spin Iron(III) Tetraphenylporphyrins

Jacek Wojaczyński, Lechosław Latos-Grażyński,* Witold Hrycyk, Ewa Pacholska, Krystyna Rachlewicz, and Ludmiła Szterenberg

Department of Chemistry, University of Wrocław, 14 F. Joliot-Curie Street, Wrocław 50 383, Poland

Received June 27, 1996[⊗]

The NMR spectra of a series of β-substituted iron(III) tetraphenylporphyrin (2-X-TPP) complexes have been studied to elucidate the relationship between the electron donating/withdrawing properties of the 2-substituent and the ^{1}H NMR spectral pattern. The electronic nature of the substituent has been significantly varied and covered the −0.6 to 0.8 Hammett constant range. Both high-spin and low-spin complexes of the general formula (2-X-TPP)Fe^{III}Cl and [(2-X-TPP)Fe^{III}(CN)$_2$]$^-$ have been investigated. The ^{1}H NMR data for the following substituents (X) have been reported: py$^+$, NO$_2$, CN, CH$_3$, BzO (C$_6$H$_5$COO), H, D, Br, Cl, CH$_3$, NH$_2$, NH$_3^+$, NHCH$_3$, OH, and O$^-$. The ^{1}H NMR resonances for low-spin dicyano complexes have been completely assigned by a combination of two-dimensional COSY and NOESY experiments. In the case of selected high-spin complexes, the 3-H resonance has been identified by the selective deuteration of all but the 3-H position. The pattern of unambiguously assigned seven pyrrole resonances reflects the asymmetry imposed by 2-substitution and has been used as an unique ^{1}H NMR spectroscopic probe to map the spin density distribution. The pyrrole isotropic shifts of [(2-X-TPP)Fe^{III}(CN)$_2$]$^-$ are dominated by the contact term. In order to quantify the substituent effect, the dependence of isotropic shift of all low-spin pyrrole resonances and 3-H high-spin pyrrole resonance versus Hammett constants has been studied. The electronic effect is strongly localized at the β-substituted pyrrole. The major change of the isotropic shift has also been noted for only one of two adjacent pyrrole rings, i.e., at 7-H and 8-H positions. These neighboring protons, located on a single pyrrole ring, experienced opposite shift changes when electron withdrawing/donating properties were modified. Two other pyrrole rings for all investigated derivatives revealed considerably smaller, substituent related, isotropic shift changes. A long-range secondary isotopic shift has been observed for [(2-D-TPP)Fe^{III}(CN)$_2$]$^-$. The effect is consistent with a general spin density distribution mechanism due to β-substitution. A fairly good correlation between the 3-H isotropic shift of (2-X-TPP)Fe^{III}Cl and the Hammett constant has been found as well. The observed contact shift pattern of [(2-X-TPP)Fe^{III}(CN)$_2$]$^-$ reflects spin π delocalization into the highest filled MO equivalent to the unsubstituted porphyrin 3e(π) orbital. To account for the substituent contribution, the semiquantitative Fenske−Hall LCAO method has been used to determine the molecular orbitals involved in the spin density delocalization. For low-spin complexes, ^{13}C pyrrole resonances of carbons bearing a proton have been identified by means of a ^{1}H−^{13}C HMQC experiment. The reversed order of ^{13}C resonance patterns as compared to their ^{1}H NMR counterparts has been determined, e.g., the largest isotropic shift of 3-H has been accompanied by the smallest measured ^{13}C isotropic shift. Analysis of the isotropic shifts in (2-X-TPP)Fe^{III}Cl and [(2-X-TPP)Fe^{III}(CN)$_2$]$^-$ suggests that the observed regularities of the electronic structure modification due to the β-substitution should apply to iron(III) natural porphyrin or geoporphyrin complexes.

Introduction

The electronic structure of iron porphyrins represents a continuously active and challenging area, especially because of the relevance of such studies to the structure and function of hemoproteins and iron porphyrin based catalytic systems. In this line of investigations ^{1}H NMR spectroscopy of paramagnetic hemoproteins and iron porphyrins provides a particularly useful tool for characterizing the oxidation/spin/ligation states of the iron.[1−3] The interaction with unpaired spin(s) at the metal induces large hyperfine shifts for the iron porphyrin substituent protons which not only permit resolution of many of the resonances in regions outside the diamagnetic envelope but allow unambiguous assignments of electronic structure based on characteristic hyperfine shift patterns for various functional groups. The hyperfine shift pattern is distinct for each oxidation/spin/ligation state of iron porphyrin. The ^{1}H NMR spectra are essentially similar but not identical for model compounds and intact hemoproteins.[3−5] The differences in the methyl resonance spread and patterns for low-spin hemoproteins and low-spin heme outside the protein crevice stimulated an extensive effort to elucidate mechanisms determining the spin density distribution of low-spin iron(III) porphyrin in general.[3] The spin density

* Author to whom correspondence should be addressed.

⊗ Abstract published in *Advance ACS Abstracts,* October 1, 1996.

(1) Bertini, I.; Turano, P.; Vila, A. J. *Chem. Rev.* **1993**, *93*, 2833.
(2) La Mar, G. N.; de Ropp, J. S. In *Biological Magnetic Resonance, NMR of Paramagnetic Molecules;* Berliner, L. J., Reuben, J., Eds.; Plenum Press: New York, 1993; Vol. 12, p 1.
(3) Walker, F. A., Simonis, U. In *Biological Magnetic Resonance, NMR of Paramagnetic Molecules*; Berliner, L. J., Reuben, J., Eds.; Plenum Press: New York, 1993; Vol. 12, p 133.
(4) Bertini, I., Luchinat, C. *NMR of Paramagnetic Molecules in Biological Systems*; Benjamin/Cummings: Reading, MA, 1986.
(5) Goff, H. M. In *Iron Porphyrins*; Lever, A. B. P., Gray, H., Eds.; Addison-Wesley: Reading, MA, 1983; p 239.
(6) (a) Traylor, T. G.; Berzinis, A. P. *J. Am. Chem. Soc.* **1980**, *102*, 2844. (b) Goff, H. M. *J. Am. Chem. Soc.* **1980**, *102*, 3252. (c) Walker, F. A. *J. Am. Chem. Soc.* **1980**, *102*, 3254. (d) Zhang, H.; Simonis, U.; Walker, F. A. *J. Am. Chem. Soc.* **1990**, *112*, 6124. (e) Walker, F. A.; Simonis, U.; Zhang, H.; Walker, J. M.; McDonald Rusciti, T.; Kipp, C.; Amptuch, M. A.; Castillo, B. V., III; Cody, S. H.; Wilson, D. L.; Graul, R. E.; Yong, G. J.; Tobin, K.; West, T. J.; Barichiewich, B. A. *New. J. Chem.* **1992**, *16*, 609.

S0020-1669(96)00772-0 CCC: $12.00

distribution in low-spin iron(III) porphyrin and derivatives can be controlled by the following factors: axial binding of planar nitrogen bases under restricted rotation conditions[6] or their mutual orientation,[7] controlled substitution at 3 and 8 positions of deuteroporphyrin;[8] the nature of the substituents and the pattern of their distribution in iron(III) octa-β-substituted porphyrin isomers,[9] substitution of *meso*-phenyl ring(s) in iron(III) tetraphenylporphyrins;[6e,10,11] mono-substitution of the β-pyrrole position of tetraphenylporphyrins;[12] saturation of pyrrole rings to form low-spin iron(III) chlorins, sulfhemins, or dioxoisobacteriochlorin[13] and by the π-acceptor character of the axial ligand.[3,7,14] Recently we have demonstrated that the five-membered isocyclic ring induced considerable asymmetry in the spin density distribution in low-spin iron(III) geoporphyrins derived from the deoxophylloerythroetioporphyrin series.[15]

In systematic studies Walker et al. have established that electronic effects controlled by substitution of *meso* phenyls plays an important role in determining the spin density distribution of low-spin *meso* substituted iron(III) tetraphenylporphyrins.[3,6e,7,10,16] In particular, the considerable differentiation of spin densities at the pyrrole-H protons within each pyrrole ring has been demonstrated.[7,10,11,16]

The intrinsic asymmetry of substituent distribution in the naturally occurring iron protoporphyrin ring is such that it is difficult to separate the relative effect of heme substituents. Moreover, the ^{1}H NMR spectra of a series of low-spin iron(III) complexes of deuteroporphyrin IX which are mono- and disubstituted at the 3 and/or 8 positions have revealed that the asymmetry of the spin density differentiation increases as the steering substituent has been chosen to be more electron withdrawing.[8] The effect at any of the four methyl positions due to 3 and 8 substituents is approximately additive. It also has been suggested that 3,8-substituted pyrrole rings lose π spin and electron density relative to the two others. However, the deuteroporphyrin structure offers only four equivalent spectroscopic probes to follow the spin density distribution around the porphyrin ring, which raises the question of their adequacy to account for the spin density distribution at each pyrrole position.

In our investigation of iron(III) geoporphyrins, identified as iron(III) etioporphyrin and its subsequent dealkylation products, we have determined that for an identical set of alkyl substituents the dramatic differences in the spin density distribution may be generated merely by reshuffling methyl, ethyl, and pyrrole resonances among eight available β-pyrrole positions.[15,17] The asymmetric modification of the pyrrole ring through N-alkylation or heteroporphyrin formation also produces the marked differences of the spin density at the *cis*-pyrrole ring.[18]

Crossley at al. have established that mono-β-substitution changes the electronic structure of tetraphenylporphyrin as revealed by alteration of the tautomeric equilibria and modulation of valence orbital levels or the modification of bond orders between β- and β'-pyrrolic position.[19] β-Substituent effects in the electroreduction of porphyrins and metalloporphyrins have been investigated as well.[20] Recently it has been demonstrated that per-β-substitution plays an instrumental role in the stabilization of highly oxidized metalloporphyrins[21a] also serving in the third generation of catalysts.[21b]

In light of this observation we have decided to study the impact of mono-β-substitution of iron(III) tetraphenylporphyrins on their ^{1}H NMR properties. The seven pyrrole protons provide the direct probe of the spin density around the porphyrin macrocycle. In principle it should allow the determination of the differences in the contact shifts for four pyrrole rings in a manner not accessible for any other porphyrin, including natural porphyrin iron(III) complexes. In order to elicit the impact of the substitutents' nature, we have chosen a series of substituents which vary systematically in their donating/withdrawing properties as measured by Hammett constants. Such an analysis has been preceded by the unambiguous resonance assignments carried out by means of two-dimensional NMR techniques.

Results and Discussion

Characterization and Spectral Assignments for High-Spin Iron(III) β-Substituted Tetraphenylporphyrin Complexes. The ^{1}H NMR data have been analyzed in the context of C_1 or C_s symmetry.

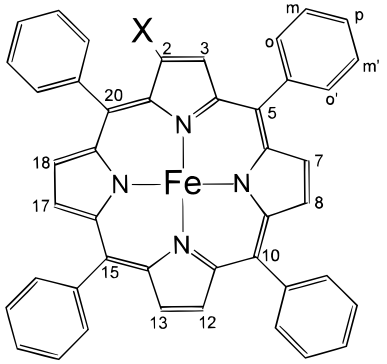

In this case there are seven distinct pyrrole positions (3, 7, 8, 12, 13, 17, 18) and four different *meso* positions (5, 10, 15, 20). With the phenyl rings in all *meso* positions it may be anticipated that the ortho and meta positions on each ring will be distinguishable due to the essentially perpendicular position between the phenyl plane and the plane of the adjacent pyrrole rings, and the restricted rotation about the *meso*-carbon-to-phenyl bond. In the case of fast rotation the number of ortho and meta

(7) (a) Walker, F. A.; Simonis, U. *J. Am. Chem. Soc.* **1991**, *113*, 8652. (b) Safo, M. K.; Walker, F. A.; Raitsimiring, A. M.; Walters, W. P.; Dolata, D. P.; Debrunner, P. G.; Scheidt, W. R. *J. Am. Chem. Soc.* **1994**, *116*, 7760.
(8) La Mar, G. N.; Viscio, D. B.; Smith, K. M.; Caughey, W. S.; Smith, M. L. *J. Am. Chem. Soc.* **1978**, *100*, 8065.
(9) Isaac, M. F.; Lin, Q.; Simonis, U.; Suffian, D. J.; Wilson, D. L.; Walker, F. A. *Inorg. Chem.* **1993**, *32*, 4030.
(10) Walker, F. A.; Balke, V. L.; McDermott, G. A. *J. Am. Chem. Soc.* **1982**, *104*, 1569.
(11) Wołowiec, S.; Latos-Grażyński, L. *Inorg. Chem.* **1994**, *33*, 3576.
(12) (a) Małek, A.; Latos-Grażyński, L.; Bartczak, T.; Żądło, A. *Inorg. Chem.* **1991**, *30*, 3223. (b) Rachlewicz, K.; Latos-Grażyński, L. *Inorg. Chem.* **1995**, *34*, 718.
(13) (a) Liccocia, S.; Chatfield, M. J.; La Mar, G. N.; Smith, K. M.; Mansfield, K. E.; Anderson, R. R. *J. Am. Chem. Soc.* **1989**, *111*, 6087. (b) Chatfield, M. J.; La, Mar, G. N.; Parker, W. O., Jr.; Smith, K. M.; Leung, H.-K.; Morris, I. K. *J. Am. Chem. Soc.* **1988**, *110*, 6352. (c) Barkigia, K. M.; Chang, C. K.; Fajer, J.; Renner, M. W. *J. Am. Chem. Soc.* **1992**, *114*, 1701.
(14) (a) Simonneaux, G.; Sodano, P. *Inorg. Chem.* **1988**, *27*, 3956. (b) Simonneaux, G.; Hindre, F.; Le Plouzennec, M. *Inorg. Chem.* **1989**, *28*, 823.
(15) Wołowiec, S.; Latos-Grażyński, L.; Serebrennikowa, O. V.; Czechowski, F. *Magn. Reson. Chem.* **1995**, *33*, 34.
(16) (a) Lin, Q.; Simonis, U.; Tipton, A. R.; Norvell, C. J. Walker, F. A. *Inorg. Chem.* **1992**, *31*, 4216. (b) Simonis, U.; Dallas, J.; Walker, F. A. *Inorg. Chem.* **1992**, *31*, 5349.
(17) (a) Bonnett, R.; Czechowski, F.; Latos-Grażyński, L. *J. Chem. Soc., Chem. Commun.* **1990**, 890. (b) Bonnett, R.; Czechowski, F.; Latos-Grażyński, L. *Energy Fuels* **1990**, *4*, 710. (c) Czechowski, F.; Latos-Grażyński, L. *Naturwissenschaften* **1990**, *77*, 578. (d) Bonnett, R.; Czechowski, F.; Latos-Grażyński, L. In *Organic Geochemistry, Advances and Applications in Energy and the Natural Environment*; Manchester University Press: Manchester, U.K., 1991; p 617. (e) Czechowski, F.; Latos-Grażyński, L.; Wołowiec, S. *Org. Geochem.* **1994**, *21*, 1059.
(18) (a) Balch, A. L.; Cornman, C. R.; Latos-Grażyński, L.; Olmstead, M. M. *J. Am. Chem. Soc.* **1990**, *112*, 7552. (b) Lisowski, J.; Latos-Grażyński, L.; Szterenberg, L. *Inorg. Chem.* **1992**, *31*, 1933.

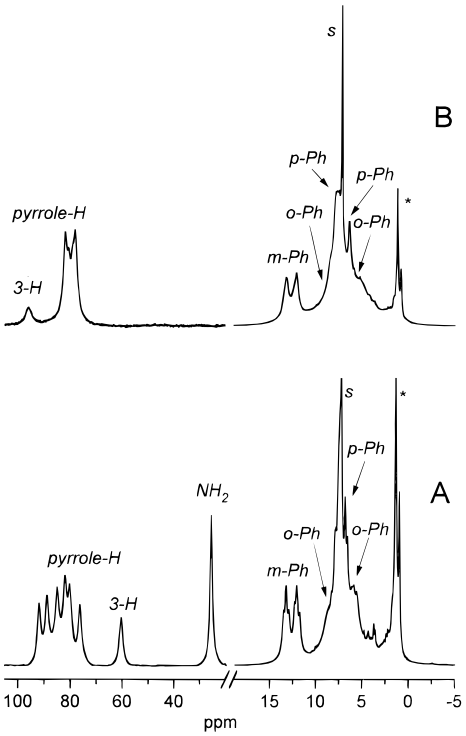

Figure 1. 300 MHz ^{1}H NMR spectra of (2-NH_2-TPP)$Fe^{III}Cl$ (trace A) and (2-NH_3-TPP)$Fe^{III}Cl_2$ (trace B) in chloroform-*d* solution at 293 K. Resonance assignments: *o*-Ph, *m*-Ph, *p*-Ph, *o*-, *m*-, and *p*-phenyl protons; NH_2, amine protons; s, solvent; *, impurities. The relative intensity of the +20 to −5 ppm region in traces A and B reduced 10 times relative to the left part of the spectrum.

resonances reduces to four. Considering the structural constraints, four para, eight ortho, and eight meta resonances may be expected for five-coordinated high-spin iron complexes since two opposite sides of the porphyrin are not equivalent. On the other hand, four ortho, four meta and four para phenyl resonances are expected for dicyano low-spin iron(III) β-substituted tetraphenylporphyrins (*vide infra*) since the molecule is symmetrical with respect to the porphyrin plane. Representative spectra of high-spin (β-NH_2-TPP)$Fe^{III}Cl$ and (β-NH_3-TPP)$Fe^{III}Cl_2$ complexes are shown in Figure 1. Resonance assignments which are given in Figure 1 and in Table 1 have been made on the basis of relative intensities, line widths, and site-specific deuteration. Direct comparisons to iron(III) tetraphenylporphyrin and previously studied (2-OH-TPP)$Fe^{III}Cl$, (2-NO_2-TPP)$Fe^{III}Cl$, (2-PPh_3-TPP)$Fe^{III}Cl_2$, [(2-O-TPP)Fe^{III}-$OH]^-$, and (2-BzO-TPP)$Fe^{III}Cl$ complexes facilitated the assignment.[12,22] Resonances of *meso* phenyls have been located in the region that is typical for high-spin iron(III) porphyrins.[3−5,23] The multiplicity of the respective resonances is directly related to the complex asymmetry. The seven unequivalent pyrrole positions should produce seven downfield shifted pyrrole resonances for well-resolved spectra. Frequently, severe overlapping reduces this number to four or five accompanied by appropriate alteration of the intensities. Their characteristic, β-substituent dependent patterns are demonstrated in Figure 2. For the sake of comparison previously reported[12,22] spectra of (2-X-TPP)$Fe^{III}Cl$ also have been included. One of the pyrrole resonances revealed remarkable sensitivity to substitution at the 2-position. This resonance varies in the 33.4−104.0 ppm range at 293 K. The other six resonances are spread near the position typical for iron(III) high-spin tetraphenylporphyrins, i.e., ca. 80 ppm (293 K). It seems plausible to assign the odd resonance to the β-substituted pyrrole ring, i.e., to the 3-H position. This thesis could be verified in part by comparison of (2-OH-TPP-d_6)$Fe^{III}Cl$ and (2-OH-TPP)$Fe^{III}Cl$ as well as [(2-O-TPP-d_6)Fe^{III}-$OH]^-$ and [(2-O-TPP)$Fe^{III}OH]^-$.

In the analogous manner the 3-H resonances of (2-CH_3O-TPP)$Fe^{III}Cl$ and (2-BzO-TPP)$Fe^{III}Cl$ have been assigned using selectively deuterated derivatives, i.e., (2-CH_3O-TPP-d_6)Fe^{III}-Cl and (2-BzO-TPP-d_6)$Fe^{III}Cl$. The selective deuteration of all but the 3-H pyrrole position has been determined[22] previously for (2-OH-TPP-d_6)$Fe^{III}Br$, leading to the suitable selective isotope labeling procedures for other derivatives. Taking advantage of the feasibility of such isotopic labeling of (2-RO-TPP)$Fe^{III}Cl$ complexes, we have proven that the β-substituent nature may be instrumental in relocating the 3-H resonance from its typical position at 80 ppm up to 11.4 ppm downfield when the substituent −OR is electron withdrawing and 46.6 ppm upfield when the substituent is electron donating.

The series of substituents BzO−, CH_3O−, −OH, and O^- has been sufficient to cover almost the full range of the accessible shift changes. With respect to the [(2-O-TPP)$Fe^{III}(OH)]^-$ one has to be aware of the axial ligand differences (OH vs Cl) which result from the synthetic requirements. In addition the contribution of the tautomeric keto form in such conditions plays some role in the determination of the shift value.[19d,22]

Similarly, (2-NH_2-TPP)$Fe^{III}Cl$ and (2-NH_3-TPP)$Fe^{III}Cl_2$ complexes, drastically different concerning their electron donating/withdrawing properties, present the 3-H resonance at two extreme positions, i.e., 58.3 and 96.2 ppm (Figure 1).

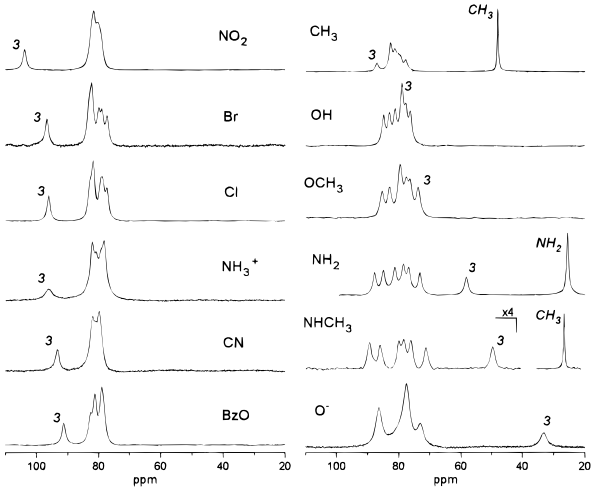

Figure 2. 300 MHz ^{1}H NMR spectra of the pyrrole region of a series of high-spin (2-X-TPP)$Fe^{III}Y$ complexes in chloroform-*d* solutions at 293 K. The respective X substituents are shown on each trace. Y = Cl for all complexes and Y = OH for [(2-O-TPP)$Fe^{III}(OH)]^-$. 3-H pyrrole resonance labeled by 3.

(19) (a) Crossley, M. J.; Harding, M. M.; Sternhell, S. *J. Am. Chem. Soc.* **1986**, *108*, 3608. (b) Crossley, M. J.; King, L. G.; Pyke, S. M. *Tetrahedron* **1987**, *43*, 4569. (c) Crossley, M. J.; Field, L. D.; Harding, M. M.; Sternhell, S. *J. Am. Chem. Soc.* **1987**, *109*, 2335. (d) Crossley, M. J.; Harding, M. M.; Sternhell, S. *J. Org. Chem.* **1988**, *53*, 1132. (e) Crossley, M. J.; Burn, P. L.; Langford, S. J.; Pyke, S. M.; Stark, A. G. *J. Chem. Soc., Chem. Commun.* **1991**, 1567. (f) Binstead, R. A.; Crossley, M. J.; Hush, N. S. *Inorg. Chem.* **1991**, *30*, 1259. (g) Crossley, M. J.; Harding, M. M.; Sternhell, S. *J. Am. Chem. Soc.* **1992**, *114*, 3266. (h) Crossley, M. J.; Harding, M. M.; Tansey, C. W. *J. Org. Chem.* **1994**, *59*, 4433.

(20) Giraudeau, A., Callot, H. J.; Jordan, J.; Ezhar, I.; Gross, M. *J. Am. Chem. Soc.* **1979**, *101*, 3857.

(21) (a) Fujii, H. *J. Am. Chem. Soc.* **1993**, *115*, 4641. (b) Ochsenbein, P.; Mandon, D.; Fischer, J.; Weiss, R.; Austin, R.; Jayaraj, K.; Gold, A.; Terner, A.; Bill, E.; Müther, M.; Trautwein, A. X. *Angew. Chem., Int. Ed. Engl.* **1993**, *32*, 1437.

(22) Wojaczyński, J.; Latos-Grażyński, L. *Inorg. Chem.* **1995**, *34*, 1044.

(23) Behere, D. V.; Birdy, R.; Mitra, S. *Inorg. Chem.* **1982**, *21*, 386.

Table 1. ^{1}H NMR Data for High-Spin β-Substituted Iron(III) Porphyrins[a]

	chemical shift (ppm)		
	pyrrole-H		
compound	3-H[b]	7-, 8-, 12-, 13-, 17-, 18-H	*m*-phenyl[c]
[(2-O-TPP)Fe^{III}(OH)]$^-$	33.4	86.5 (2H), 77.4 (3H), 73.0	*d*
(2-NHCH$_3$-TPP)Fe^{III}Cl[e]	49.4 (41.6)	89.4, 86.0, 80.1, 78.4, 76.0, 71.4	13.5, 13.2, 13.1, 12.7, 12.3, 12.1, 11.9, 11.5
(2-NH$_2$-TPP)Fe^{III}Cl[f]	58.3 (50.5)	88.0, 85.0, 81.5, 78.7, 76.8, 73.3	13.5, 13.2 (2H), 12.9, 12.3, 12.1 (2H), 11.8
(2-OCH$_3$-TPP)Fe^{III}Cl[g]	74.0 (66.3)	85.4, 83.1, 79.6 (2H), 77.7, 76.3	13.5, 13.3 (2H), 13.1, 12.3, 12.1−11.9 (3H)[h]
(2-OH-TPP)Fe^{III}Cl[i]	79.1 (70.9)	85.0, 83.1, 81.3, 79.1, 77.8, 76.4	13.6, 13.2 (2H), 13.0, 12.5, 12.0 (2H), 11.8
(2-CH$_3$-TPP)Fe^{III}Cl[j]	87.2 (78.6)	82.7 (2H), 81.3, 80.4, 80.4, 79.6	13.4 (3H), 13.2, 12.2 (3H), 12.0
(2-BzO-TPP)Fe^{III}Cl[k]	91.4 (82.7)	82.8, 81.3 (2H), 79.1 (2H), 78.5	13.3 (4H), 12.2 (3H), 11.9
(2-CN-TPP)Fe^{III}Cl	93.3 (83.9)	82.0 (2H), 81.0, 79.8 (3H)	13.6 (2H), 13.4, 13.2, 12.4 (2H), 12.3, 12.1
(2-PPh$_3$-TPP)Fe^{III}Cl$_2$[l]	95.6 (86.5)	84.2, 81.3, 80.2, 78.7, 76.1 (2H)	12.9 (4H), 12.4 (2H), 11.5 (2H)
(2-NH$_3$-TPP)Fe^{III}Cl$_2$	96.2	82.1 (2H), 80.9, 79.3, 78.4 (2H)	13.3 (4H), 12.2 (4H)
(2-Cl-TPP)Fe^{III}Cl	96.4 (87.7)	83.0, 82.0 (2H), 79.5, 78.9, 77.5	13.3 (4H), 12.2 (4H)
(2-Br-TPP)Fe^{III}Cl	96.7 (87.8)	82.4 (3H), 80.0, 79.0, 77.3	13.3 (4H), 12.3 (4H)
(2-py-TPP)Fe^{III}Cl$_2$[m]	103.7 (94.3)	82.7, 80.5 (3H), 78.2, 77.4	12.9 (4H), 12.6 (4H)
(2-NO$_2$-TPP)Fe^{III}Cl	104.0 (94.9)	81.8 (3H), 80.3 (3H)	13.6 (3H), 13.4, 12.5 (3H), 12.2

[a] All spectra recorded in chloroform-*d* at 293 K. Signal intensity different from 1H given in parentheses. [b] Isotropic shift given in parentheses.[19a,39] [c] *o*-Phenyl and *p*-phenyl resonances in the 5−8 ppm region. [d] Overlapped with strong solvent signal. [e] CH$_3$ resonance at 25.6 ppm, NH peak at −1.6 ppm. [f] NH$_2$ resonance at 25.5 ppm. [g] OCH$_3$ signal at ca.12 ppm. [h] Overlapped with OCH$_3$ peak. [i] OH resonance at 16.0 ppm.[22] [j] CH$_3$ signal at 48.0 ppm. [k] Benzoyloxy resonances: *o*-H, 9.1 ppm (2H); *m*-H, 8.2 ppm (2H); *p*-H, 8.0 ppm.[22] [l] 298 K; β-substituent resonances in the 7.2−8.5 ppm region.[12a] [m] Pyridine resonances: *o*-H, 10.8 ppm (2H); *m*-H, 10.9 ppm (2H); *p*-H, 9.2 ppm.[12b]

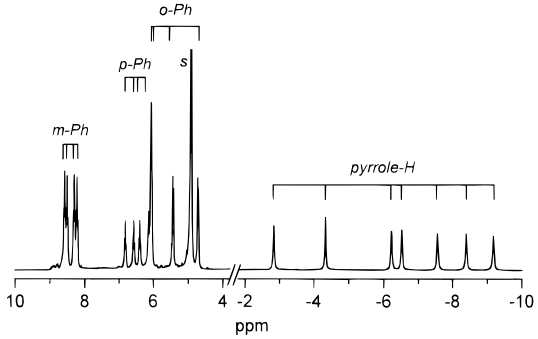

Figure 3. 300 MHz ^{1}H NMR spectrum of [(2-CN-TPP)Fe^{III}(CN)$_2$]$^-$ in methanol-d_4 solution at 293 K. Resonance assignments follow those of Figure 1.

Spectral Characterization of Low-Spin Iron(III) β-Substituted Porphyrins. Addition of an excess of potassium cyanide to a solution of (2-X-TPP)Fe^{III}Cl in methanol-d_4 results in its conversion to a six-coordinate low-spin complex: [(2-X-TPP)Fe^{III}(CN)$_2$]$^-$. Usually low-spin iron(III) porphyrins, formed by coordination of two cyanide ligands, result in very narrow paramagnetically shifted resonances due to the optimal relaxation properties.[24] This property even allowed direct detection of a scalar multiplet structure in paramagnetic systems.[8,18]

The representative ^{1}H NMR spectrum for [(2-CN-TPP)Fe^{III}(CN)$_2$]$^-$ is shown in Figure 3. A comparison of all pyrrole patterns is presented in Figures 4 and 5 and Table 2. The characteristic sets of seven upfield shifted pyrrole resonances observed for each compound investigated is of importance for describing the electronic fine structure. These resonances are accompanied by sets of upfield shifted ortho and para *meso*-phenyl proton resonances and downfield shifted meta protons.

In our case the primary assignment could be made on the basis of the position of resonances, their intensities, and scalar multiplet structure. The full assignment required an application of two-dimensional ^{1}H NMR techniques. Two-dimensional COSY and NOESY experiments have been shown to be effective in connecting pyrrole proton resonances in low-spin iron(III) complexes of *meso*-substituted tetraphenylporphyrins.[11,16] Within each non-equivalent pyrrole ring the pyrrole protons are expected to be scalar coupled with an approximate 5 Hz coupling constant.[19] Figure 6 presents the COSY spectrum for the representative low-spin β-substituted iron(III) complex, i.e., [(2-Br-TPP)Fe^{III}(CN)$_2$]$^-$. Cross-peaks reveal pairwaise scalar coupling between protons located on the same pyrrole ring. The unique resonance without correlation to any other pyrrole resonance could be unambiguously assigned to the 3-H proton of the β-substituted ring. Similarly we could easily separate phenyl signals into four subsets, each assigned to individual *meso*-phenyls. The unambiguous assignment of the

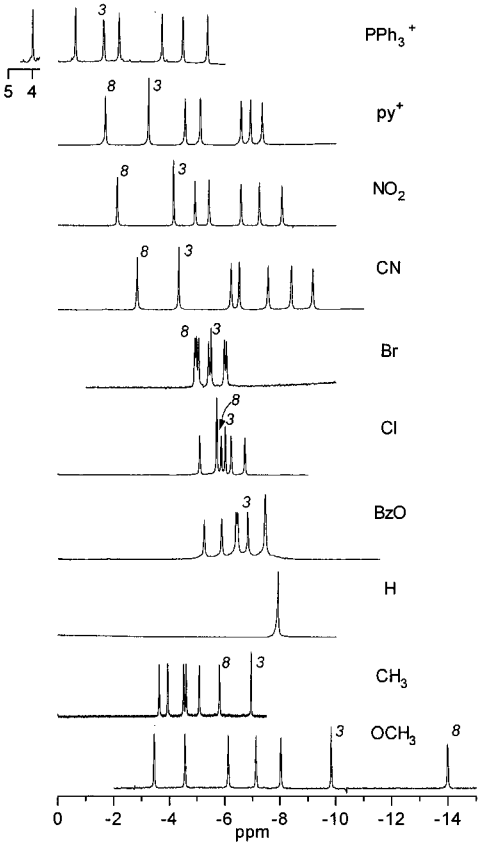

Figure 4. 300 MHz ^{1}H NMR spectra of the pyrrole region of a series of low spin [(2-X-TPP)Fe^{III}(CN)$_2$]$^-$ complexes in methanol-d_4 solutions at 293 K. X substituents marked on each trace. The most characteristic 3-H and 8-H pyrrole resonances labeled by 3 and 8, respectively.

(24) La Mar, G. N.; Del Gaudio, J., Frye, J. S. *Biochim. Biophys. Acta* **1977**, *498*, 422.

Table 2. ^{1}H NMR Data for Low-Spin β-Substituted Iron(III) Porphyrins[a]

	chemical shift (ppm)																			
	pyrrole-H							ortho-Ph				meta-Ph				para-Ph			
compound	3	7	8	12	13	17	18	5	10	15	20	5	10	15	20	5	10	15	20
[(2-O-TPP)Fe^{III}(CN)$_2$]$^{2-}$ [b]	−44.0	*c*	−37.0			*c*				*d*				*d*				*d*	
[(2-NH$_2$-TPP)Fe^{III}(CN)$_2$]$^-$	−31.0	−2.3	−19.8	−4.9	−9.8	−2.5	−6.7	8.2	4.0	7.6	4.2	8.4	6.8	8.7	7.1	7.3	6.1	7.2	6.4
	(−38.8)	(−11.0)	(−28.5)	(−13.7)	(−18.6)	(−11.2)	(−15.2)	(0.0)	(−3.9)	(−1.5)	(−3.5)	(0.6)	(−1.0)	(0.9)	(−0.7)	(−0.5)	(−1.7)	(−0.6)	(−1.4)
[(2-NHCH$_3$-TPP)Fe^{III}(CN)$_2$]$^-$ [e]	−27.2	−0.8	−21.5	−4.5	−8.6	−2.7	−6.2	8.4	3.8	7.9	4.0	8.6	6.7	8.8	7.1	7.4	6.0	7.4	6.4
	(−35.0)	(−9.4)	(−30.2)	(−13.2)	(−17.3)	(−11.4)	(−14.6)	(0.2)	(−4.1)	(−1.3)	(−3.3)	(0.8)	(−1.1)	(1.0)	(−0.7)	(−0.4)	(−1.8)	(−0.4)	(−1.4)
[(2-OH-TPP)Fe^{III}(CN)$_2$]$^-$ [b]	−20.8	*f*	−17.9			*f*				*d*				*d*				*d*	
	(−29.2)		(−26.7)																
[(2-OCH$_3$-TPP)Fe^{III}(CN)$_2$]$^-$ [g]	−10.0	−3.4	−14.3	−7.3	−6.2	−4.6	−8.2	7.1	4.3	6.7	4.5	8.6	7.6	8.7	7.1	7.0	6.0	6.8	6.4
	(−17.7)	(−12.2)	(−23.1)	(−16.1)	(−15.0)	(−13.4)	(−16.9)	(−1.1)	(−3.9)	(−1.5)	(−3.5)	(0.9)	(−0.1)	(1.0)	(0.0)	(−0.7)	(−1.7)	(−0.9)	(−1.3)
[(2-CH$_3$-TPP)Fe^{III}(CN)$_2$]$^-$ [h]	−7.0	−3.6	−5.8	−3.9	−4.6	−5.1	−4.5	5.8	5.6	5.8	6.0	8.5	8.5	8.6	8.4	6.5	6.4	6.5	6.9
	(−15.6)	(−12.4)	(−14.6)	(−12.8)	(−13.5)	(−13.9)	(−13.1)	(−2.4)	(−2.6)	(−2.4)	(−2.1)	(0.8)	(0.8)	(0.9)	(0.7)	(−1.2)	(−1.3)	(−1.2)	(−0.8)
[(2-BzO-TPP)Fe^{III}(CN)$_2$]$^-$ [b]	−6.9	{−5.3 and −7.5, −5.9 and −7.5, −6.4 and −6.5}								*d*				*d*				*d*	
	(−15.6)																		
[(2-Cl-TPP)Fe^{III}(CN)$_2$]$^-$	−6.0	−5.7	−5.8	−5.7	−6.2	−5.1	−6.7	5.6	5.5	5.8	5.7			8.3−8.5[i]		6.5	6.4	6.5	6.8
	(−14.7)	(−14.6)	(−14.7)	(−14.5)	(−15.0)	(−13.9)	(−15.5)	(−2.6)	(−2.7)	(−2.4)	(−2.4)			(0.6−0.8)		(−1.2)	(−1.3)	(−1.2)	(−0.9)
[(2-Br-TPP)Fe^{III}(CN)$_2$]$^-$	−5.4	−5.3	−4.8	−4.9	−5.9	−4.9	−5.9	5.4	5.6	5.8	5.9			8.4−8.6[i]			6.4−6.5[i]		6.9
	(−14.3)	(−14.2)	(−13.7)	(−13.7)	(−14.7)	(−13.8)	(−14.7)	(−2.8)	(−2.6)	(−2.4)	(−2.2)			(0.6−0.8)			(−1.4−−1.3)		(−0.9)
[(2-CN-TPP)Fe^{III}(CN)$_2$]$^-$	−4.3	−9.2	−2.8	−6.5	−8.4	−6.2	−7.6	4.7	6.1	5.4	6.1	8.4	8.6	8.3	8.6	6.2	6.6	6.4	6.8
	(−13.7)	(−18.1)	(−11.7)	(−15.2)	(−17.1)	(−15.1)	(−16.6)	(−3.5)	(−2.1)	(−2.8)	(−2.1)	(0.6)	(0.8)	(0.5)	(0.8)	(−1.6)	(−1.2)	(−1.4)	(−1.0)
[(2-NO$_2$-TPP)Fe^{III}(CN)$_2$]$^-$	−4.2	−8.1	−2.1	−5.4	−7.2	−4.9	−6.6	4.8	6.0	5.3	5.9	8.6	8.8	8.5	8.8	6.2	6.5	6.3	6.5
	(−13.3)	(−17.0)	(−11.0)	(−14.1)	(−15.9)	(−13.8)	(−15.6)	(−3.4)	(−2.2)	(−2.9)	(−2.4)	(0.9)	(1.1)	(0.8)	(1.1)	(−1.5)	(−1.2)	(−1.4)	(−1.2)
[(2-py-TPP)Fe^{III}(CN)$_2$][j]	−3.2	−7.3	−1.7	−5.1	−6.9	−4.6	−6.6	4.8	5.9	5.5	6.0	8.6	8.8	8.5	8.5	6.1	6.5	6.4	6.5
	(−12.5)	(−16.2)	(−10.6)	(−14.0)	(−15.8)	(−13.2)	(−15.4)	(−3.4)	(−2.3)	(−2.7)	(−2.0)								
[(2-PPh$_3$-TPP)Fe^{III}(CN)$_2$][b,k]	−1.5	{−5.3 and −0.5, −2.1 and −3.6, −4.3 and 4.1}						{3.6, 5.2, 6.0, 6.4}				{8.6, 8.8, 9.0, 9.8}				{5.5, 6.2, 6.6, 6.6}			
	(−10.6)																		

[a] All spectra recorded in methanol-d_4 at 293 K. Isotropic shifts given in parentheses below measured resonance positions.[19a,39] [b] Full resonance assignment not achieved. [c] Not all resonances identified; another pyrrole signals at −7.9, −1.7, and −1.5 ppm. [d] Signals not identified. [e] Assignment based on COSY spectrum and on comparison to results obtained for 2-NH$_2$− complex. Methyl resonance at 21.3 ppm. [f] Not all resonances identified; another pyrrole peak at −3.9 ppm. [g] OCH$_3$ signal at 4.6 ppm (isotropic shift 0.6 ppm). [h] CH$_3$ resonance at 11.4 ppm (isotropic shift 8.8 ppm). [i] Overlapping resonances. [j] Pyridine resonances at 7.5, 8.3, and 8.8 ppm. [k] Substituent signals at 6.8, 7.2, and 7.5−7.8 ppm.

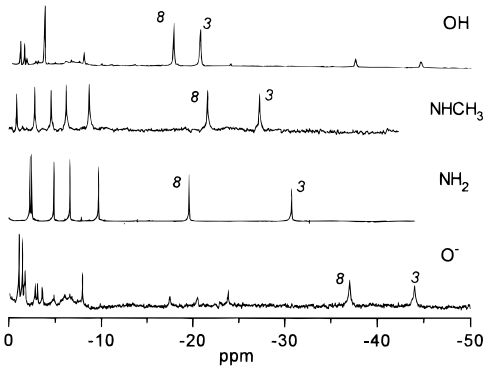

Figure 5. 300 MHz ^{1}H NMR spectra of the pyrrole region of a series of low-spin [(2-X-TPP)Fe^{III}(CN)$_2$]$^-$ complexes in methanol-d_4 solutions at 293 K; X, strongly electron donating substituent, OH, NHCH$_3$, NH$_2$, O$^-$. The sample where [(2-OH-TPP)Fe^{III}(CN)$_2$]$^-$ dominates was obtained by dissolution of (2-OH-TPP)Fe^{III}Cl in methanol-d_4 saturated with KCN, the deprotonation product of [(2-OH-TPP)Fe^{III}(CN)$_2$]$^-$, i.e., [(2-O-TPP)Fe^{III}(CN)$_2$]$^{2-}$ was obtained in a similar manner starting from [(2-O-TPP)Fe^{III}]$_3$.

3-H resonance provided convincingly a starting point for the further individual assignment by means of the NOESY experiment. The representative NOESY map is demonstrated in the lower box of Figure 6. The observed scalar and dipolar connectivities are depicted in the lower part of Figure 6.

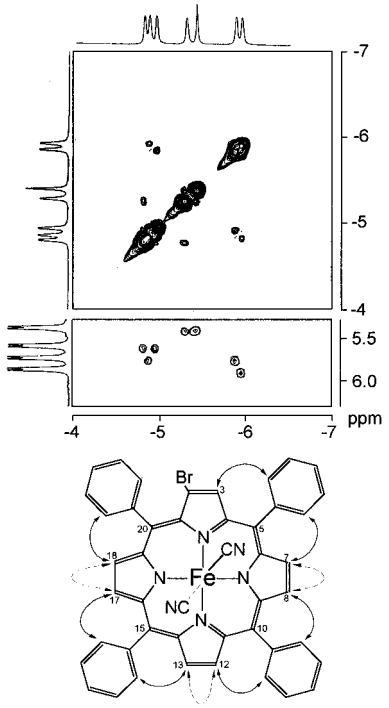

Figure 6. 2D ^{1}H NMR spectra of [(2-Br-TPP)Fe^{III}(CN)$_2$]$^-$ in methanol-d_4 solution at 293 K. The upper box presents the COSY map of the pyrrole region, while the lower one shows a fragment of NOESY spectrum with cross-peaks derived from contacts of *o*-phenyl and pyrrole protons. These contacts are indicated by solid arrows in the molecule scheme. Dashed arrows correspond to COSY cross-peaks. Two ortho protons on each phenyl ring are equivalent.

All required cross-peaks have been identified in the two-dimensional maps. Analogous procedures of assignments for low-spin iron(III) porphyrins have been carried out for all species under investigation with the exception of [(2-BzO-TPP)Fe^{III}(CN)$_2$]$^-$, [(2-OH-TPP)Fe^{III}(CN)$_2$]$^-$, and [(2-O-TPP)Fe^{III}(CN)$_2$]$^{2-}$. Complicated equilibria have been encountered in titration of (2-OH-TPP)Fe^{III}Cl or [(2-O-TPP)Fe^{III}]$_3$ in methanol-d_4 with potassium cyanide. The gradual hydrolysis of [(2-BzO-TPP)Fe^{III}(CN)$_2$]$^-$ to produce [(2-O-TPP)Fe^{III}(CN)$_2$]$^{2-}$ and related derivatives excluded lengthy NOESY experiments for this complex. However, the COSY experiment resulted in identification of the 3-H resonance which is distinct because it is not scalar coupled to any other pyrrole resonances. Its identification has been confirmed by comparison of [(2-BzO-TPP)Fe^{III}(CN)$_2$]$^-$ and [(2-BzO-TPP-d_6)Fe^{III}(CN)$_2$]$^-$ spectra. The deuteration procedure has been used to assign 3-H resonances of [(2-OH-TPP)Fe^{III}(CN)$_2$]$^-$ and [(2-O-TPP)Fe^{III}(CN)$_2$]$^{2-}$.

Apart from pyrrole and phenyl resonances we have also assigned the corresponding resonances of β-substituents for [(2-CH$_3$O-TPP)Fe^{III}(CN)$_2$]$^-$, [(2-CH$_3$-TPP)Fe^{III}(CN)$_2$]$^-$, and [(2-NHCH$_3$-TPP)Fe^{III}(CN)$_2$]$^-$ (Table 2). 2-CH$_3$ and 2-CH$_3$O signals are located in predictable regions based upon the number of bonds separating the resonating protons from the pyrrole ring.[3] In particular the downfield position of 2-CH$_3$ resonance in [(2-CH$_3$-TPP)Fe^{III}(CN)$_2$]$^-$ (11.4 ppm) presents a similar value but of the opposite sign as the corresponding pyrrole protons. This behavior is typical for low-spin iron(III) porphyrins.[3,8]

The assignment of the 2-CH$_3$ resonance results also from the COSY experiment where the cross-peak correlating the 2-CH$_3$ and 3-H resonances has been identified. The scalar coupling in this moiety $^4J_{CH_3,H}$ which is a requisite of this cross-peak varies in the range 1.14−1.45 Hz.[19g] On the other hand, the position of the NH−*CH$_3$* resonance in [(2-NHCH$_3$-TPP)Fe^{III}(CN)$_2$]$^-$ (21.3 ppm) does not have precedence assuming the similar pattern of the spin delocalization in the following fragments: β-CH$_2$−*CH$_3$* and β-NH−*CH$_3$*. The typical chemical shift for the −CH$_2$−*CH$_3$* resonance at 301 K equals 0.3 ppm as exemplified by low-spin iron(III) etioporphyrin complexes.[17a] In fact, the high-spin spectrum of (2-NHCH$_3$-TPP)Fe^{III}Cl also demonstrates the methyl resonance at relatively large downfield chemical shift (25.6 ppm) as compared to 6.7 ppm of β-CH$_2$−*CH$_3$* in (OEP)Fe^{III}Cl at 298 K.[25]

Analysis of Isotropic Shift of High-spin Iron(III) β-Substituted Tetraphenylporphyrin Complexes. The electron configuration of the high-spin iron ($S = {}^5/_2$) gives a ^{6}A ground electronic state for which **g** tensor is isotropic. However, the zero field splitting (ZFS) generates a dipolar shift proportional to ZFS.[26,27] This dipolar contribution at the pyrrole position is notably smaller in the (TPP)Fe^{III}X (X = Cl, Br, I) series than the contact one and varies in the 7 −14% range of the overall isotropic shift, depending on the axial ligand.[23] The phenyl resonances (meta and para) in the investigated series demonstrated an alternation of the isotropic shift, although their absolute values are smaller for the para position relative to the meta ones. This is consistent with contribution of the contact shift combined with marked addition of the downfield dipolar part.[23,27] We would like to point out that the observed resonances of the *meso* substitutents do not change their position considerably upon β-substitution (Table 1). We have assumed that the dipolar contribution in the series remains constant. The observed changes of the isotropic shift must result from the contact mechanisms. One has to notice that both axial or rhombic components of the dipolar shift would not generate changes of the isotropic shifts located in the case of high-spin iron porphyrins, mostly on a single pyrrole ring or on two selected protons of two cis pyrrole rings as determined for low-spin iron porphyrins (vide infra).

Considering the pyrrole resonance pattern (Figure 2, Table 1), we have noticed a considerable dependence of the 3-H

(25) Balch, L.; Latos-Grażyński, L.; Noll, B. C.; Olmstead, M. M. *Inorg. Chem.* **1992,** *31*, 2248.
(26) Kurland, R. J.; McGarvey, B. R. *J. Magn. Reson.* **1970**, *2*, 286.
(27) La Mar, G. N.; Walker, F. A. *J. Am. Chem. Soc.* **1973**, *95*, 6950.

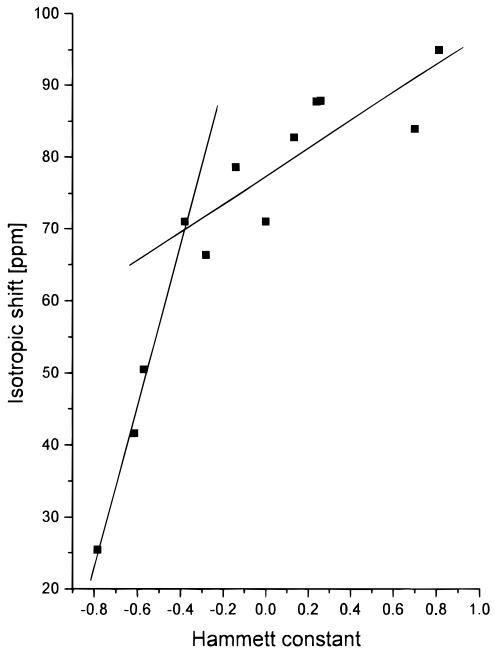

Figure 7. Plot of the isotropic shift of 3-H pyrrole proton for high-spin (2-X-TPP)$Fe^{III}Cl$ complexes vs the Hammett σ constant of substituent X (293 K). Lines are illustrative only.

resonance on the electron donating/withdrawing properties of the 2-X substituent. The relevant dependence of the isotropic shift versus the respective Hammett constants[28] is presented in Figure 7. The plot presents smooth although not necessarily linear changes of the isotropic shift vs the Hammett constants. For the sake of clarity we present this and the following trends using the straight lines. In general, the electron donating substituent produces an upfield relocation of the 3-H proton when the downfield direction has been determined for electron withdrawing ones. Both relocations have been referred to the symmetrical (TPP)$Fe^{III}Cl$ complex. Although the specific assignments could not be made for the remaining pyrrole positions, we have found that the electron donating substitutents produce the largest spread of the pyrrole resonances. They are consistently centered around the typical 80 ppm position (Table 1).

Analysis of Isotropic Shifts of Dicyano Low-spin Iron(III) β-Substituted Tetraphenylporphyrin Complexes. In order to analyze the contact shift of dicyano low-spin iron(III) β-substituted tetraphenylporphyrin complexes, we have to evaluate the dipolar contribution. The *meso*-phenyl resonances of paramagnetic metalloporphyrins have been shown to yield characteristic shift patterns that depend on whether the contact or dipolar shift dominates.[29] Alternation of the shift direction is characteristic if a contact shift dominates. The predominant dipolar shift is determined by a symmetry of the magnetic susceptibility tensor and the geometric factors. In the typical case of the axial symmetry the shift of phenyl resonances is in one direction and decreases in the order ortho > meta ≈ para. Considering the isotropic shifts of *meso*-phenyls of dicyano complexes of iron(III) β-substituted porphyrins, we have noticed that the scalar mechanism dominates in the whole molecule. The relative values of the phenyl isotropic shifts are close to the cases where the contact shift clearly predominates, i.e., $[(TPP)Fe^{III}(CN)_2]^-$, $[(TPP)Fe^{III}(R\text{-}NC)_2]^+$, or $[(TPP)Fe^{III}(R\text{-}py)_2]^+$ if the R choice assures strong π-acceptor properties of the R-pyridine ligand.[7b,14b,24] Recently Safo et al. attributed this observation to the composed ground electronic state which evolves from $(d_{xy})^2(d_{xz}d_{yz})^3$ to $(d_{xz}d_{yz})^4(d_{xy})^1$, depending on the π-acceptor properties of the axial ligand.[7b] Previously it was also argued that the cyanide complexes of iron(III) porphyrins in methanol solution are involved in hydrogen bonding which leads to lowering of a dipolar term.[24]

The axial part of the dipolar contribution is uniform in all directions. Therefore, it cannot be the essential source of the pyrrole resonances differentiation. As a matter of fact, the phenyl resonances for complexes with electron withdrawing substituents present very similar isotropic shift values in structurally different positions. The marked in plane anisotropy of the phenyl shifts has been noticed only for the derivatives with electron donating substituents (NH_2, $NHCH_3$, OCH_3). For the $[(2\text{-}NH_2\text{-}TPP)Fe^{III}(CN)_2]^-$ complex the 10- and 20-phenyls presented upfield isotropic shifts for all (ortho, meta, para) positions. The 5,15-phenyls revealed a shift of alternate signs, but the values deviated from the pattern assigned above to the contact contribution. This observation is consistent with some rhombic contribution to the dipolar shift of the *meso*-phenyl according to the second term in the formula[29]

$$(\Delta\nu/\nu_0)^{dip} = (1/(3N))[\chi_{zz} - {}^1/_2(\chi_{xx} + \chi_{yy})](3\cos^2\theta - 1)/r^3 + (1/(2N))[(\chi_{xx} - \chi_{yy})\sin^2\theta\cos(2\Omega)/r^3] \quad (1)$$

where N is the Avogadro number; χ_{ii}, the principal components of the magnetic susceptibility tensor; θ, the angle between the z molecular axis and the proton−metal vector; r, the length of this vector; and Ω, the angle between projection of this vector on the xy plane and the x axis.

The rhombic term imposes a well-defined relationship on this contribution; namely, 10- and 20-phenyl resonances which are related by 180° rotation should exhibit the identical shift due to the rhombic term. In addition 5,15-phenyl related to 10,20-phenyls by 90° must have equal dipolar shifts but in the opposite directions. It seems that this contribution qualitatively accounts for the *meso*-phenyl shift of $[(2\text{-}NH_2\text{-}TPP)Fe^{III}(CN)_2]^-$. Small differentiation of the isotropic shift noticed for the phenyl resonances of $[(2\text{-}NO_2\text{-}TPP)Fe^{III}(CN)_2]^-$ may result from the rhombic contribution as well, although in this case 5,15-phenyls present larger changes which may reflect the reorientation of the magnetic susceptibility tensor.

Even for the extreme examples, i.e., $[(2\text{-}NH_2\text{-}TPP)Fe^{III}(CN)_2]^-$ and $[(2\text{-}NO_2\text{-}TPP)Fe^{III}(CN)_2]^-$ the dipolar contribution as the major reason of the pyrrole resonances differentiation may be ruled out. The axial contribution, if essential, adds uniformly to each β-proton shift. The rhombic term would contribute pairwaise as seen already for the *meso*-phenyls, e.g., 3−13 (in the same direction) and 3−8 (in the opposite direction). In particular, the 3-H and 8-H behaviors do not comply with such an expectation. We conclude that the spread of the β-H resonances reflects primarily the modification of the spin density distribution.

To quantify the effects, we have plotted in Figure 8 the isotropic shift of the most substituent sensitive 3-H and 8-H pyrrole resonances vs Hammett constants as previously done for the high-spin state. In addition the correlation between differences of the isotropic shifts within one pyrrole ring (i.e., 7-H and 8-H shifts) vs the β-substituent Hammett constant has been found. Similar approaches have been explored concerning several physicochemical parameters of phenyl substituted iron(III) tetraphenylporphyrins.[6e,10,31] A good fit between β-sub-

(28) Exner, O. In *Correlation Analysis in Chemistry*; Shorter, J., Chapman, N. B., Eds.; Plenum Press: New York and London, 1978; p 439.
(29) Goff, H. M.; La Mar, G. N. *J. Am. Chem. Soc.* **1977**, *99*, 6599.
(30) Jesson, J. P. In *NMR of Paramagnetic Molecules;* La Mar, G. N.; Horrocks, W. D.; Holm, R. H., Eds.; Academic Press: New York, 1973; p 18.

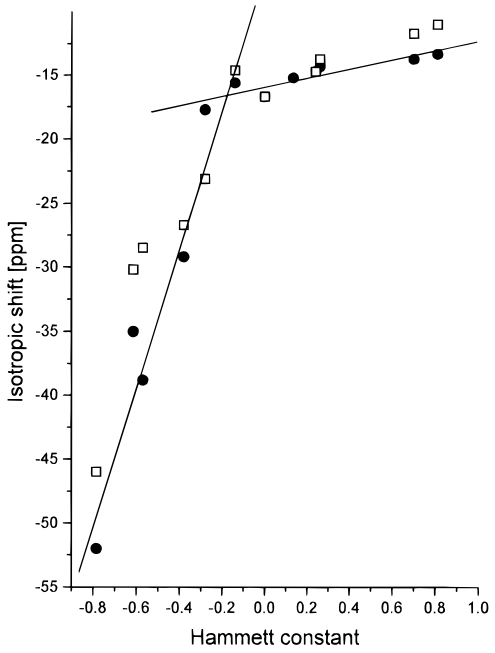

Figure 8. Plot of the isotropic shift of pyrrole protons for low-spin $[(2\text{-X-TPP})Fe^{III}(CN)_2]^-$ complexes vs the Hammett constant of substituent X (293 K). Filled circles correspond to 3-H, and squares, to 8-H. Lines are illustrative only.

stituent Hammett constants and the half-wave potentials for the first oxidation and the first reduction potentials of β-substituted copper(II) tetraphenylporphyrins was previously established.[19f,20]

As is apparent from the data in Table 2, pyrrole resonances show different sensitivities regarding the 2-substitution. The electronic effect is mostly localized at the β-substituted pyrrole. However, the major change of the isotropic shift has been noted also for only one of two cis pyrrole rings, namely, that one which carries 7-H and 8-H protons. Two other pyrrole rings revealed considerably smaller isotropic shift changes. The respective values vary between limits which can be conveniently demonstrated by two relevant compounds, i.e., $[(2\text{-}NO_2\text{-TPP})Fe^{III}(CN)_2]^-$ and $[(2\text{-}NH_2\text{-TPP})Fe^{III}(CN)_2]^-$ (Table 2). From examinations of the $[(2\text{-}NH_2\text{-TPP})Fe^{III}(CN)_2]^-$ isotropic shifts we can split a set of pyrrole resonances into two subsets. The first subset contains the 3-H, 8-H, 13-H, and 18-H resonances; the second one includes 7-H, 12-H, and 17-H. The protons in each subset are related by a 4-fold symmetry in their maternal unsubstituted compound, i.e., $[(TPP)Fe^{III}(CN)_2]^-$. The absolute values of the upfield contact shift decrease in the order 3-H > 8-H $\gg$ 13-H > 18-H in the first case and 12-H > 17-H > 7-H in the second one. Generally, the isotropic shifts in the first group are larger than in the second one. The second limiting case $[(2\text{-}NO_2\text{-TPP})Fe^{III}(CN)_2]^-$ demonstrates the different order of the subset shifts, i.e., 8-H < 3-H < 18-H < 13-H and 17-H < 12-H < 7-H, but the overall pattern is even more complicated (8-H < 3-H < 17-H < 12-H < 18-H < 13-H < 7-H) as both sets do overlap. Other compounds under investigation provide suitable examples of the intermediate patterns related to the electron donating/withdrawing properties of their substituents.

The largest changes of the isotropic shifts found for 3-H, 8-H (in one direction) and 7-H (in the opposite direction) allowed us to conclude that the dependence of the isotropic shift vs the Hammett constants can be described as composed from two linear segments differentiated by their slopes. The electron donating section seems to be more substituent sensitive. We attribute this folding of the Hammett plot to the change in the mechanism of the electron density transmission. The substituents with the strongly negative Hammett constants may involve the resonance contribution apart from the inductive one. We would like to emphasize that the β-substitution can generate considerable shift differentiation within each pyrrole ring. Such a shift difference for the 7-H - 8-H couple achieves the largest value for two extreme cases discussed above and changes almost linearly depending on the Hammett constants. This parameter reverses sign beginning from $[(2\text{-Br-TPP})Fe^{III}(CN)_2]^-$.

Finally, a comparison of the average shift of each pyrrole ring, i.e., 7, 8-H, 12, 13-H, and 17, 18-H couples, may reflect modification of the electron density distribution between four pyrroles of the macrocycle. These values increase by ca. 6 ppm for the 7,8-H couple, going from $[(2\text{-}NO_2\text{-TPP})Fe^{III}(CN)_2]^-$ to $[(2\text{-}NH_2\text{-TPP})Fe^{III}(CN)_2]^-$ ($[(TPP)Fe^{III}(CN)_2]^-$ not included). The other pyrrole rings demonstrated scattered variation of the averaged value but their spread has not exceeded the 3.0 ppm (12,13-H) and 2.0 ppm (17,18-H) range, respectively. In the case of electron withdrawing substituents the pyrrole averaged isotropic shift increased in the series 7,8-H < 12,13-H $\approx$ 17,18-H (for $[(2\text{-}NO_2\text{-TPP})Fe^{III}(CN)_2]^-$). The reversed relation has been generated by electron donating substitutents, i.e., 7,8-H > 12,13-H > 17,18-H (for $[(2\text{-}NH_2\text{-TPP})Fe^{III}(CN)_2]^-$). The order of the average pyrrole shifts clearly reflected the relation to the electronic structure.

Isotope Shifts in the ^{1}H NMR Spectrum of Mono-β-deuterated Iron(III) Tetraphenylporphyrin. The ^{1}H NMR spectroscopy of β-substituted iron porphyrins has already given evidence of being a very sensitive tool to probe the fine details of the electronic structure. To explore the limits of the method, we have attempted to examine the effect of replacing a single β-H proton by deuterium.

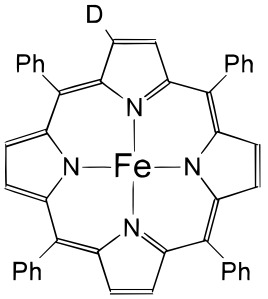

Such a replacement has resulted in the observable changes of the pyrrole resonance seen in the ^{1}H NMR spectrum of $[(2\text{-D-TPP})Fe^{III}(CN)_2]^-$ shown in Figure 9. We have attributed the change to the secondary isotope shift. The figure demonstrates the resolution enhanced spectrum to emphasize the spectral pattern. A multiplet of pyrrole resonances is composed of three signals at -7.495, -7.510, and -7.550 ppm. A well-defined singlet resonance has been found for the $[(TPP)Fe^{III}(CN)_2]^-$ species under identical conditions. Addition of nondeuterated species enhanced the most downfield resonance (Figure 9, upper trace). The secondary isotopic effect equals 0.000, -0.010, and -0.055 ppm for the -7.495, -7.510, and -7.550 ppm resonances. The pyrrole pattern is consistent with a long-range isotope effect which extends over all macrocyclic positions. The resonances of *meso*-phenyls (not shown) have not presented the isotope substitution related changes.

(31) (a) Walker, F. A.; Lo, M.-W.; Ree, M. T. *J. Am. Chem. Soc.* **1976**, *98*, 5552. (b) Walker, F. A.; Benson, M. *J. Phys. Chem.* **1982**, *86*, 3495. (c) Walker, F. A.; Reis, D.; Balke, V. L. *J. Am. Chem. Soc.* **1984**, *106*, 6888. (d) Balke, V. L.; Walker, F. A.; West, J. T. *J. Am. Chem. Soc.* **1985**, *107*, 1226.

(32) Medforth, C. J.; Shiau, F.-Y.; La Mar, G. N.; Smith, K. M. *J. Chem. Soc., Chem. Commun.* **1991**, 590.

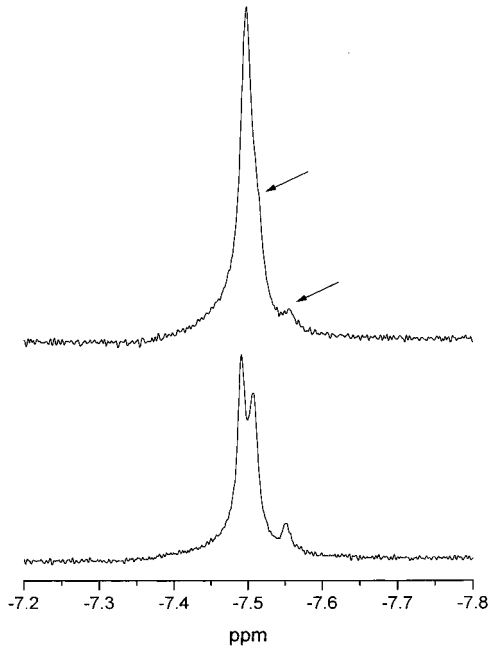

Figure 9. Pyrrole region of 300 MHz ^{1}H NMR spectrum of [(2-D-TPP)Fe^{III}(CN)$_2$]$^-$ in methanol-d_4 solution at 293 K (lower trace) and of the same sample to which [(TPP)Fe^{III}(CN)$_2$]$^-$ has been added (upper trace). The resolution enhancement has been applied to both spectra. Arrows at the upper trace indicate features resulting from the secondary isotopic effect.

The long-range isotope effect was previously determined in the ^{1}H NMR spectra of low-spin deuterated natural hemes.[32] It seems reasonable to assume that the 3-proton next to 2-deuterium undergoes the largest secondary isotopic shift leading to a tentative assignment of the most upfield shifted resonance at 7.550 ppm to the 3-H position. Several mechanisms may be involved to account for the secondary isotopic shift.[32,33] We suggest that the observed changes due to the isotope effect can be explained by a transmission of electron effects in a similar manner to any other β-substituent investigated in this paper. Previously it was indicated that deuterium behaves as an electron donor. The substituent parameters are equal, $\sigma_I = -0.001$ and $\sigma_R = -0.0001$, with respect to protium.[34] Considering the sign and value of the Hammett constant, the expected pattern of pyrrole resonances may resemble the one established for [(2-CH$_3$-TPP)Fe^{III}(CN)$_2$]$^-$ with the largest upfield displacement for the 3-H resonance.

The feasible primary isotopic effect can be in principle evaluated as the difference of shifts found in the ^{1}H NMR spectrum of [(TPP)Fe^{III}(CN)$_2$]$^-$ and ^{2}H NMR spectrum of [(2-D-TPP)Fe^{III}(CN)$_2$]$^-$. The effect is in the error limits determined by broadening of the 2-D pyrrole resonance in the ^{2}H NMR spectrum.

Assignment of ^{13}C β-Pyrrole Resonances. ^{1}H reverse detection in heteronuclear correlation spectroscopy (HMQC) of paramagnetic iron porphyrins provides the scalar hetero correlation under natural abundance conditions of ^{13}C.[35] In the system under investigation, namely, low-spin iron porphyrins [(2-X-TPP)Fe^{III}(CN)$_2$]$^-$, the correlation technique offers a route for identifying β-pyrrole resonances, taking advantage of the fact that the full assignment of the ^{1}H signals of the β-^{13}C$-^1$H pairs has been established already.

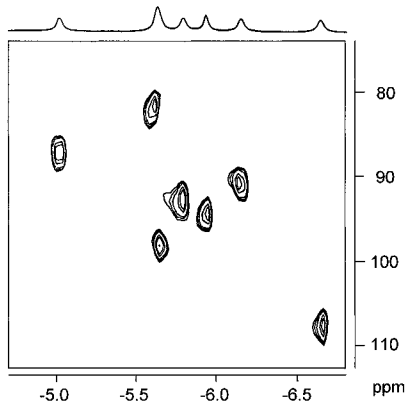

Figure 10. The pyrrole region of the 300 MHz ^{1}H$-^{13}$C HMQC spectrum of [(2-Cl-TPP)Fe^{III}(CN)$_2$]$^-$ in methanol-d_4 solution at 293 K.

An example of a HMQC ^{1}H$-^{13}$C map, measured for [(2-Cl-TPP)Fe^{III}(CN)$_2$]$^-$, is demonstrated in Figure 10. The spectrum correlates the shift of β-pyrrole carbons in the F_1 dimension with the shift of the attached protons in the F_2 dimension. The β-carbons are observed in the map as cross-peaks with coupled protons. The ^{13}C pyrrole chemical shifts are gathered in Table 3. Generally, upfield isotropic shifts of ^{13}C resonances have been found. The composed nature of the ^{13}C isotropic shift renders a direct analysis of the spin density distribution difficult.[36] However, we find it necessary to comment that we have noticed *the reversed order* of ^{13}C resonances in comparison to their ^{1}H NMR counterparts. This effect has been the most pronounced for 3-CH, 7-CH, and 8-CH fragments. The monotonic increase of the 7-C chemical shifts vs the Hammett constant accompanied by the monotonic decrease of the 8-C chemical shifts has been observed. These trends are opposite to those found for the corresponding ^{1}H shifts.

As the metal-centered dipolar shift for low-spin iron(III) porphyrins is relatively small, we may assume that the isotropic shift is expressed by a formula

$$(\Delta\nu/\nu_0)^{LC}{}_\beta + (\Delta\nu/\nu)^{con}{}_\beta = D\rho^\pi{}_\beta + [(S + 2Q_{CC'} + Q_{CH})\rho^\pi{}_\beta + Q_{C'C}(\rho^\pi{}_{\beta 1} + \rho^\pi{}_\alpha)][|\gamma_e/\gamma_c|S(S+1)/3kT] \quad (2)$$

where $\rho^\pi{}_\beta$, $\rho^\pi{}_{\beta 1}$, and $\rho^\pi{}_\alpha$ are the spin densities at the carbon of interest and the neighboring carbons, S and Q_{xy} are proportionality constants reflecting different polarization pathways which influence the resultant isotropic shift, and D describes the carbon-centered dipolar effect. Other symbols have their usual meaning. Taking the S and Q values analogously as in radical systems,[36] we may simplify the equation

$$(\Delta\nu/\nu_0)^{LC}{}_\beta + (\Delta\nu/\nu)^{con}{}_\beta = [99.7\rho^\pi{}_\beta - 39(\rho^\pi{}_{\beta 1} + \rho^\pi{}_\alpha)](|\gamma_e/\gamma_c|S(S+1)/3kT) + D\rho^\pi{}_\beta \quad (3)$$

We find that the second term (neighboring term) of the opposite sign may dominate the observed isotropic shift providing that $\rho^\pi{}_\beta \gg \rho^\pi{}_{\beta 1}$, $\rho^\pi{}_\alpha$ which is usually the case for 8-C and 7-C positions when electron donating substitutents are involved.

(33) (a) Horn, R. R.; Everett, G. W., Jr.; *J. Am. Chem. Soc.* **1971**, *93*, 7175. (b) Hebendanz, N.; Kohler, F. H.; Scherbaum, F.; Schlesinger, B. *Magn. Reson. Chem.* **1989**, *27*, 798. (c) Heintz, R. A.; Neiss, T. G.; Theopold, K. H. *Angew. Chem., Int. Ed. Engl.* **1994,** *33*, 2326.

(34) (a) Young, W. R.; Yannoni, C. S. *J. Am. Chem. Soc.* **1969**, *91*, 4581. (b) Streitwieser, A., Jr.; Humprey, J. S., Jr. *J. Am. Chem. Soc.* **1967**, *89*, 3767.

(35) (a) Yamamoto, Y.; Fujii, N. *Chem. Lett.* **1987,** 1703. (b) Yamamoto, Y.; Nanai, N.; Inoue, Y.; Chujô, R. *Bull. Chem. Soc. Jpn.* **1989**, *62*, 1773. (c) Simonis, U.; Tan, H.; Walker, F. A. *J. Inorg. Biochem.* **1993**, *51*, 145. (d) Banci, L.; Bertini, I.; Pierattelli, Vila, A. J. *Inorg. Chem.* **1994,** *33*, 4338. (e) Santos, H.; Turner, D. L. *Eur. J. Biochem.* **1992**, *206*, 721. (f) Turner, D. L. *Eur. J. Biochem.* **1993**, *211*, 563.

(36) Goff, H. M. *J. Am. Chem. Soc.* **1981**, *103*, 3714, and references cited therein.

Table 3. ^{13}C NMR Pyrrole Shifts for Low-Spin β-Substituted Iron(III) Porphyrins[a]

compound	δ (ppm)						
	3-C	7-C	8-C	12-C	13-C	17-C	18-C
$[(2\text{-}NH_2\text{-}TPP)Fe^{III}(CN)_2]^-$	171.0	11.0	132.0	53.0	144.5	80.0	78.0
$[(2\text{-}OCH_3\text{-}TPP)Fe^{III}(CN)_2]^-$	79.5	50.5	126.0	76.5	100.0	89.0	95.5
$[(2\text{-}CH_3\text{-}TPP)Fe^{III}(CN)_2]^-$ [b]	94.0	79.5	96.0	80.0	89.0	91.0	87.0
$[(2\text{-Cl-TPP})Fe^{III}(CN)_2]^-$	93.0	97.0	91.5	81.5	89.5	86.0	106.5
$[(2\text{-Br-TPP})Fe^{III}(CN)_2]^-$	95.5	99.0	89.0	80.0	89.0	87.0	105.0
$[(2\text{-}NO_2\text{-}TPP)Fe^{III}(CN)_2]^-$	78.5	127.0	70.0	77.5	83.5	83.0	119.0
$(2\text{-py-TPP})Fe^{III}(CN)_2$	83.5	127.0	70.5	78.0	87.0	83.0	118.0

[a] Measured in methanol-d_4 at 293 K; for $[(TPP)Fe^{III}(CN)_2]^-$ ^{13}C pyrrole shift equals 89.0 ppm. Diamagnetic positions of 7-, 8-, 12-, 13-, 17-, and 18-C resonances for these compounds vary in a small range and are found in the 130−140 ppm region. [b] 2-*C*H$_3$ resonance at −8.0 ppm.

Thus, the relation $\rho^{\pi}_{\beta} \gg \rho^{\pi}_{\beta 1}$ implies $|\delta_{\beta}(^1H)| > |\delta_{\beta 1}(^1H)|$ but $|\delta_{\beta}(^{13}C)| < |\delta_{\beta 1}(^{13}C)|$.

Analysis of π-Density Delocalization Mechanisms. The typical delocalization pathways for high-spin iron(III) tetraphenylporphyrins produce the pyrrole resonances strongly downfield shifted as a result of the σ-contact contribution due to the delocalization through a σ-framework by way of a σ-donation to the half occupied $d_{x^2-y^2}$ iron(III) orbital. Additionally the π-delocalization locates a considerable amount of spin density at the *meso* positions.[3,23] The mechanism is identified as Fe → porphyrin π back-bonding and involves empty 4e(π*) orbitals of the porphyrin with the large contribution of $2p_z$ *meso* carbon atomic orbitals. The π spin density delocalized further on produces sign alternation of the contact shift measured for the *meso*-phenyl resonances and is reflected by large upfield shift of *meso* protons of $(OEP)Fe^{III}Cl$.

Considering the typical delocalization scheme in terms of the orbitals derived for D_{4h} symmetry of the porphyrin ring, we have excluded 4e(π*) orbitals as instrumental in determination of the contact shift variation for the β-substituted derivatives. Simply the expected amount of spin density at the β-pyrrole positions of the 4e(π*) orbitals is too small. We have already noticed that β-substitution changed negligibly the position of the *meso* resonances, which can be roughly treated as the measure of the 4e(π*) contribution in the π-mechanism. Earlier, based solely upon $(2\text{-}NO_2TPP)Fe^{III}Cl$ and $(2\text{-}PPh_3TPP)Fe^{III}Cl_2$, we had suggested that β-substitution changes the efficiency of the σ-delocalization mechanism particularly at the β-substituted pyrrole.[12] Although such a mechanism may contribute to the overall mechanism, we will suggest here that the variation of the pyrrole positions in the ^{1}H NMR spectrum requires a specific π-delocalization mechanism.

In the case of low-spin iron(III) porphyrins the spin density is delocalized from $(d_{xz}d_{yz})^3$ orbitals into the filled 3e(π) orbitals of the porphyrins by porphyrin to iron π back-bonding. The 3e(π) orbitals are characterized by large coefficients at β-pyrrole positions, and the spin density distribution for low-spin iron porphyrins is usually related to their pattern. This approach formally valid for the D_{4h} symmetry was applied with qualitative success to a large variety of metalloporphyrins of lower symmetry.[3−5] At this stage of discussion we may conclude that the contact shift of high-spin iron (III) β-substituted tetraphenylporphyrins may result from the simultaneous delocalization in σ as well as both filled 3e(π) and vacant 4e(π*) molecular orbitals. Usually for high-spin iron(III) porphyrins the upfield π contribution due to delocalization at 3e(π) orbitals may be overshadowed by the strong downfield contribution of the σ-mechanism. In our particular case of the β-substituted derivatives this new route seems to be of importance. To explore this hypothesis the plot of high-spin iron(III) porphyrin vs isotropic shift of its low-spin counterpart have been analyzed. The fairly monotonic correlation (not shown) supports the view that *the similar* π-spin density mechanism accounts for the

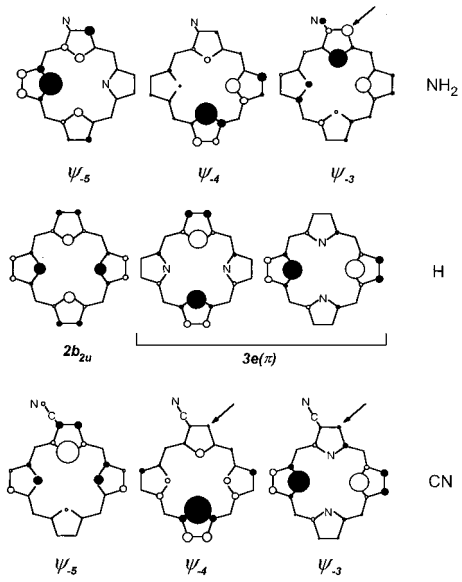

Figure 11. Symmetry properties of the filled π porphyrin orbitals that have proper symmetry and energy to overlap with d_{xz} and d_{yz} orbitals of Fe(III) ion. Phases are indicated by unshaded and filled circles with the size corresponding to unpaired spin density. The orbitals of interest for 2-aminoporphyrin (highest trace) and 2-cyanoporphyrin (lowest trace) reflect the influence of the electron donating/withdrawing substituent. Energy of orbitals increases from left to right. The orbital numbering is chosen with respect to the HOMO (ψ_{-1}) according to decreasing energy. Arrows indicate the most characteristic differences. For the sake of comparison $2b_{2u}$ and 3e(π) orbitals of regular porphyrin are presented in the middle trace.

upfield relocation of the 3-H resonances for both spin states as the electron donating properties of the substituent increases. Obviously the β-substitutions have affected the patterns of the molecular orbitals involved in the spin density transfer. The orbitals adequate for D_{4h} symmetry require a reasonable modification.

To account at least qualitatively for the β-substituent contribution, the semiquantitative Fenske−Hall LCAO method has been applied.[37] The idealized geometry of the porphyrin dianions has been used in this calculation.[38] The occupied molecular orbitals with symmetry and energy related to the 3e(π) and $2b_{2u}$ orbitals of the unperturbed system are presented in Figure 11. The calculations have been carried out for all 2-X substituents under investigation, but only the extreme situations as far as electron donor/withdrawing properties, i.e., $2\text{-}NH_2$ and 2-CN, are presented. The $2\text{-}NH_2$ group is oriented in such a way that the free electron pair is in the plane perpendicular to the porphyrin plane. For the sake of comparison, the 3e(π) and $2b_{2u}$ orbitals of unsubstituted porphyrin calculated by the Fenske−Hall approach are included in the figure as well.

(37) Hall, M. B.; Fenske, R. F. *Inorg. Chem.* **1972**, *11*, 768.
(38) Scheidt, W. R.; Lee, Y. J. *Struct. Bonding* **1987**, *64*, 1.

Instead of two, as for the high symmetry system, three π-orbitals need to be considered. Each of the sets presents the proper symmetry and energy to effectively overlap with the d_{xz}, d_{yz} orbitals of the iron(III). We have noticed that in both cases the orbitals of the highest energy in the group present consistently very large (2-NH_2) or very small (2-CN) function coefficients at 3-C, as expected based upon ^{1}H NMR investigation for both high-spin and low-spin iron(III) porphyrins. However, the calculated orbital coefficients at other pyrrole positions do not correctly predict the experimental order of resonances. Definitely the more sophisticated approach is required to reproduce in detail the spin density distribution. From the model presented it is obvious that several π routes must simultaneously contribute to the outcome of the spin density distribution.

The calculations predict properly the downfield shift of the 2-N-CH_3 resonance of $[(2\text{-}NHCH_3\text{-}TPP)Fe^{III}(CN)\}_2]^-$. The 2-N nitrogen orbital is involved in the π-orbital of the porphyrin. The π spin density at this atom induces the unusual downfield shift of the CH_3 substituent as expected for the π-delocalization pattern.

Conclusions

This work broadens our understanding of the mechanisms of the π spin density distribution in high-spin and low-spin iron(III) tetraphenylporphyrins and their β-substituted derivatives. One- and two-dimensional studies resulted in unambiguous assignment of all resonances of low-spin complexes. These identified β-H resonances could be used as unique probes to map simultaneously the delocalization of unpaired electrons at seven positions of the porphyrin macrocycle. It has become apparent that the localized perturbation at the 2-C position has been transmitted all over the porphyrin macrocycle with the largest effect experienced at 3-H and 7-H, 8-H positions, i.e., at the modified position and at only one from two adjacent pyrrole rings.

The pyrrole resonances could be divided into two groups, related by a pseudo-4-fold symmetry, i.e., {3-H, 8-H, 13-H, 18-H} and {7-H, 12-H, 17-H}, based upon the $\beta-$substituent effects. The absolute values of the upfield contact shift decrease (clockwise) in the order 3-H > 8-H $\gg$ 13-H > 18-H in the first case and 12-H > 17-H > 7-H in the second one for the most electron donating substituents. Generally, the isotropic shifts in the first group are larger than in the second one. The different order of the shifts, i.e., 8-H < 3-H < 18-H < 13-H and 12-H < 17-H < 7-H seems to be adequate for description of electron withdrawing systems. In addition the neighboring protons of the ring adjacent to the substituted one, namely, 7-H and 8-H, experienced opposite changes when electron withdrawing/donating properties of the sustituent are modified.

In the related case of dicyano iron(III) 3,8-deuteroporphyrin IX complexes monosubstituted at 3- or 8- position, the ligand structure provided only four equivalent probes of the spin density, i.e., four methyl groups.[8] Porphyrin ring substituents seemed to simply rearrange spin density among the four *pyrrole rings*. In such an approach the pyrrole ring substituted by an electron donating substituent was supposed to receive more spin density as manifested by the larger value of the methyl contact shift and smaller shifts of other methyls. However, the isotropic shifts of dicyanoiron(III) complexes 3- or 8- monoacetyl-substituted 3,8-deuteroporphyrin IX follow the regularity revealed in our investigations; e.g., a substitution at the 3-position by electron withdrawing acetyl decreases the shift of 2-CH_3 but increases the shift of 18-CH_3 resonance. The discussed methyls are mutually located similar to the 3-H and 7-H pyrrole protons of 2-substituted tetraphenylporphyrins, and *the effect of the opposite sign may be typical for these positions*. Analyzing an example of 7-H and 8-H contact shifts of $[(2\text{-X-TPP})Fe^{III}(CN)_2]^-$, a contradictory opinion could be offered for the same pyrrole ring concerning the efficiency of the spin density distribution among pyrrole rings. The conclusion would depend solely on the choice of a probe. In our opinion the β-substitution controls the spin density pattern simultaneously effecting two sets of pyrrole resonances (each set component from a different pyrrole ring) as opposed to the view where each pyrrole ring is treated as a unit.

Finally, we have demonstrated that the isotropic 3-H shift changes of high-spin and low-spin iron(III) complexes presented an identical trend depending on the nature of the substituent. This reveals a spin delocalization due to P $\rightarrow$ Fe π bonding. Thus, this mechanism which is widely accepted for low-spin iron(III) porphyrins also accounts for a constituent isotropic shift of high-spin derivatives.

Experimental Section

Methanol-d_4 (Glaser AG) has been used as received. Chloroform-*d* (Glaser AG) was dried before use by passing through basic alumina.

***β*-Substituted 5,10,15,20-tetraphenylporphyrins.** 2-Pyridiniumyl-5,10,15,20-tetraphenylporphyrin,[12b] 2-nitro-5,10,15,20-tetraphenylporphyrin,[12a,20,39,40] 2-cyano-5,10,15,20-tetraphenylporphyrin,[20,41] 2-methyl-5,10,15,20-tetraphenylporphyrin,[19h] 2-bromo-5,10,15,20-tetraphenylporphyrin,[20,41] 2-chloro-5,10,15,20-tetraphenylporphyrin,[20] 2-amino-5,10,15,20-tetraphenylporphyrin,[42] 2-benzoyloxy-5,10,15,20-tetraphenylporphyrin,[22,41] 2-methoxy-5,10,15,20-tetraphenylporphyrin,[41,43] 2-benzoyloxy-5,10,15,20-tetraphenylporphyrin-d_7,[22] the symmetrical 5,10,15,20-tetraphenylporphyrin,[45] and 5,10,15,20-tetraphenylporphyrin-d_8 deuterated at all pyrrole positions[46] have been synthesized using known procedures.

Insertion of iron followed a known route.[22]

(2-$NHCH_3$-TPP)$Fe^{III}Cl$ was obtained by methylation of (2-NH_2-TPP)$Fe^{III}Cl$ with methyl iodide.

(2-NH_3-TPP)$Fe^{III}Cl_2$ was produced by adding HCl in chloroform-*d* to the chloroform-*d* solution of (2-NH_2-TPP)$Fe^{III}Cl$.

(2-OH-TPP)$Fe^{III}Cl$, $[(2\text{-O-TPP})Fe^{III}(OH)]^-$, (2-OH-TPP-$d_6$)$Fe^{III}Cl$, $[(2\text{-O-TPP-}d_6)Fe^{III}OH]^-$ were generated from the trimeric derivatives $[(2\text{-O-TPP})Fe^{III}]_3$ or $[(2\text{-O-TPP-}d_6)Fe^{III}]_3$ as recently reported.[22]

The benzoylation with benzoyl chloride or methylation with methyl iodide of (2-OH-TPP-d_6)$Fe^{III}Cl$ yielded (2-BzO-TPP-d_6)$Fe^{III}Cl$ and (2-CH_3O-TPP-d_6)$Fe^{III}Cl$, respectively.

The mono-β-deuteration of $TPPH_2$ was carried out using the procedure elaborated by Crossley and King[44] The extent of deuteration as evaluated by integration of ^{1}H NMR spectrum of 2-D-$TPPH_2$ yielded ca. 90%, which corresponds to about 1−2% of nondeuterated material ($TPPH_2$) in the whole sample.

Usually, the dicyano-ligated complexes of the investigated iron(III) porphyrin were prepared by dissolution of 2−3 mg of the respective high-spin complex in 0.4 mL of methanol-d_4 saturated with KCN. For several compounds, namely, for 2-NO_2, 2-py^+, 2-BzO, 2-OH, and 2-O^- derivatives, an excess of potassium cyanide led to side reactions (caused by cyanide acting as a reductant, a nucleofilic agent, or a base). To eliminate them, the saturated solution of KCN in methanol-d_4 was added to the methanol-d_4 solution of high-spin complex in minimal amount sufficient for conversion to the dicyano complex.

NMR Experiments. ^{1}H NMR spectra were recorded on a Bruker AMX spectrometer operating in the quadrature mode at 300 MHz. The

(39) Shine, H. J.; Padilla, A. G.; Wu, S. M.; *J. Org. Chem.* **1979**, *23*, 4069.
(40) Catalano, M. M.; Crossley, M. J.; Harding, M. M.; King, L. G. *J. Chem. Soc., Chem. Commun.* **1984**, 1535.
(41) Callot, H. *Bull. Soc. Chim. Fr*. **1974**, 1492.
(42) Baldwin, J. E.; Crossley, M. J.; DeBernadis, J. F. *Tetrahedron* **1982**, *38*, 685.
(43) Catalano, M. M.; Crossley, M. M.; King, L. G. *J. Chem. Soc., Chem. Commun.* **1984**, 1537.
(44) Crossley, M. J.; King, L. *J. Org. Chem.* **1993**, *58*, 4370.
(45) Lindsey, J. S.; Schreiman, I. C.; Hsu, H. C.; Kearney, P. C.; Marguerettaz, A. M. *J. Org. Chem.* **1987**, *52*, 827.
(46) Boersma, A. D.; Goff, H. M. *Inorg. Chem.* **1982**, *21*, 581.

residual ^{1}H NMR resonances of the deuterated solvents ($CHCl_3$ or CHD_2OD) were used as a secondary reference. Magnitude COSY spectra of $[(2\text{-X-TPP})Fe^{III}(CN)_2]^-$ were obtained after collecting the standard 1D reference spectra. The 2D COSY spectra were usually collected by use of 1024 points in t_2 over desired bandwidth (to include all desired peaks) with 256 t_1 blocks and 40−200 scans per block in which 4 dummy scans were included. Repetition time was 150 ms in all cases. Prior to Fourier transformation, the 2D matrix was multiplied in each dimension with a 30° shifted sine-bell squared window function and zero filled to obtain a 1024 × 1024 word square matrix. The NOESY (NOESYTP) spectra of $[(2\text{-X-TPP})Fe^{III}(CN)_2]^-$ were accumulated by use of 1024 points in t_2 and 512 in t_1 and 200 scans per t_1 block. Prior to Fourier transformation the 2D matrix was multiplied in each dimension with a 30° shifted sine-bell squared window function and zero-filled to obtain a 1024 × 1024 word square matrix. Experimental parameters were varied to obtain the best resolution in the signal to noise mode. Usually the repetition time was equal 150 ms. The mixing time was varied in the 80−120 ms range. The NOESY spectra were processed in the phase-sensitive or magnitude modes. Both COSY and NOESY spectra were acquired at 293−295 K unless the temperature lowering was required to produce better separation of resonances.

The ^{1}H−^{13}C HMQC spectra were accumulated by use of 1024 points in t_2 and 128 in t_1 and 32−256 scans per t_1 block. A relaxation delay of 150 ms was used, and the $\Delta = 1/2J$ refocusing delay was set to 3.2 ms.

Acknowledgment. The financial support of the State Committee for Scientific Research KBN (Grant 2 2651 92 03) is kindly acknowledged.

IC960772P